

# Active Deformation of the Arabian Plate and its Margins

Michael Floyd<sup>1</sup>, Abdullah ArRajehi<sup>2</sup>, Robert King<sup>1</sup>, Simon McClusky<sup>3</sup>, Robert Reilinger<sup>1</sup>, Mohamad Douad<sup>4</sup>, Jamal Sholan<sup>5</sup>, Firyal Bou-Rabee<sup>6</sup>

1. Department of Earth, Atmospheric and Planetary Sciences, Massachusetts Institute of Technology, Cambridge, MA 02139, USA  
 2. King Abdulaziz City for Science and Technology, Riyadh, Saudi Arabia  
 3. Research School of Earth Sciences, Australian National University, Canberra, ACT, Australia  
 4. National Earthquake Center, Damascus, Syrian Arab Republic  
 5. Seismological & Volcanological Observatory Center, Dhahar, Yemen  
 6. Geology Department, Kuwait University, Kuwait City, Kuwait

AGU Fall Meeting 2012

Abstract G53A-1125

## Summary

We present a new GPS velocity field for Arabia and surrounding areas based on observations from 1994 to 2012 (Figure 1, 7A, B, C, D). While internal Arabia plate deformation is small and marginally significant in comparison to the rate of Arabia-Eurasia convergence (Figure 2), the improved resolution of GPS observations are beginning to provide constraints on strain internal to the plate (Figure 3). Geodetic velocities in the plate tectonic reference frame for Arabia show a systematic westward motion that increases for sites along the eastern side of the Arabian Plate (Figure 4). The overall trend is consistent with slowing of AR-NU relative motion (see GPS and plate tectonic Euler vectors, Figure 5D). The spatial distribution of strain cannot be resolved from the sparse available data, but compressional strain appears to characterize the eastern part of the plate. Apparent compression extends > 200 km west of the Zagros Fold and Thrust Belt that forms the eastern, collisional boundary of the Arabian plate with Eurasia (Iran) (Figure 7C, D). Broad-scale contraction of the Arabian plate seems intuitively reasonable given that the east and north sides of the plate are dominated by active continental collision (Zagros, E. Turkey/Caucasus) while the west and south sides are bordered by mid-ocean ridge spreading (Red Sea and Gulf of Aden).

## GPS velocities

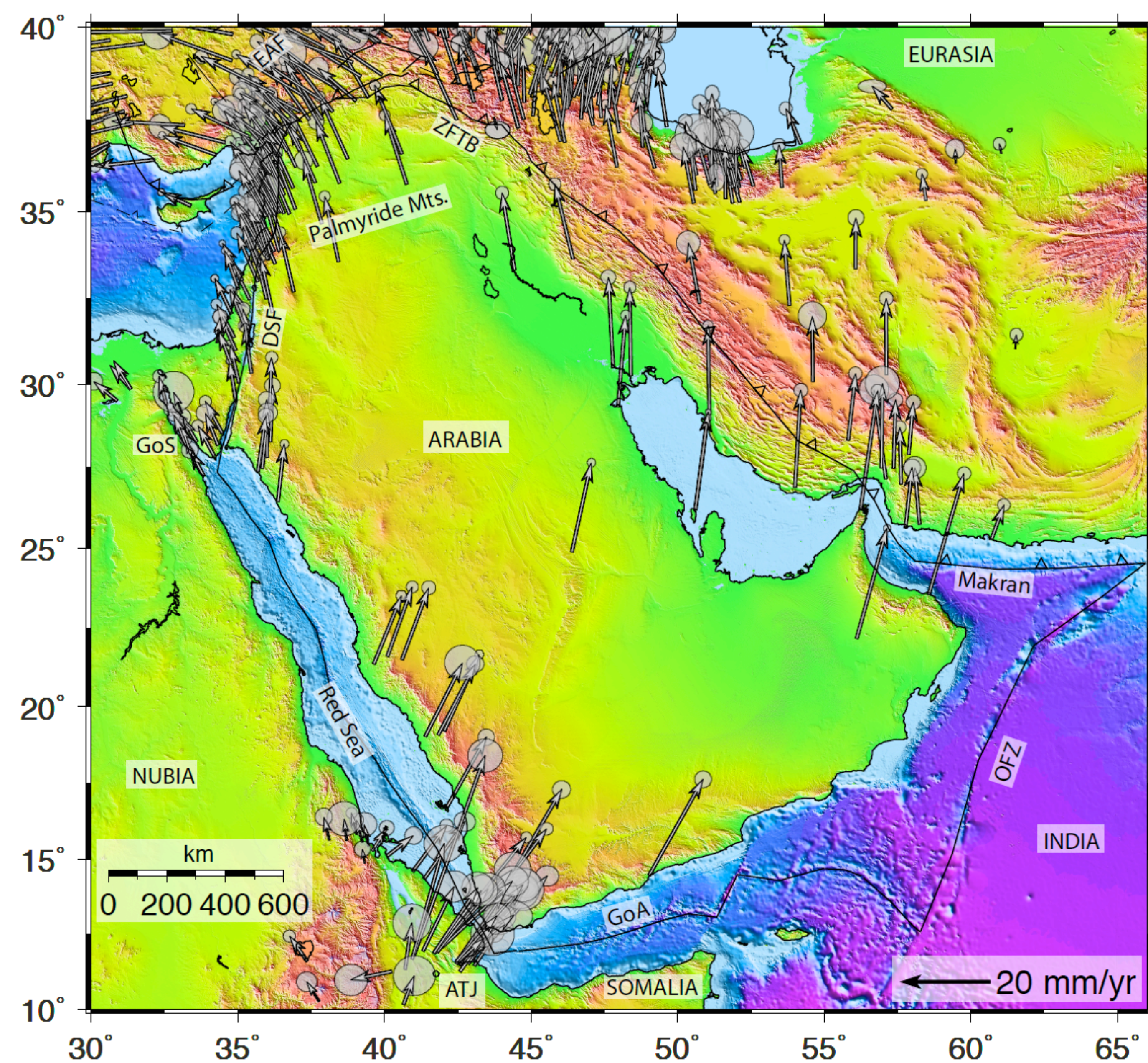


Figure 1 GPS velocities and 95% confidence ellipses for the Arabian Plate and surrounding areas with respect to Eurasia.

Figure 3 → Principal strain rates derived from GPS velocities. Area is divided into bins of 8 degrees by 8 degrees.

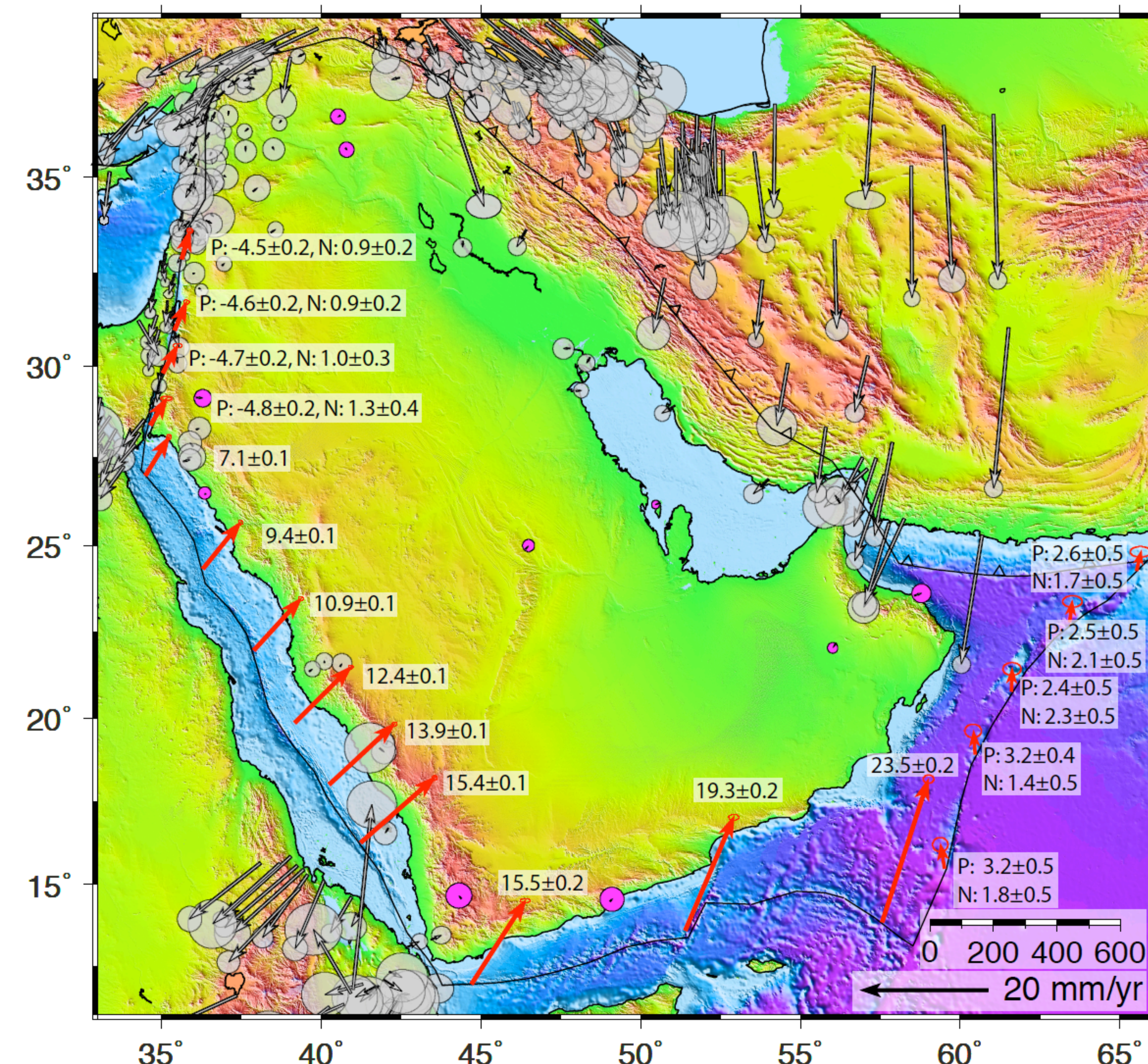
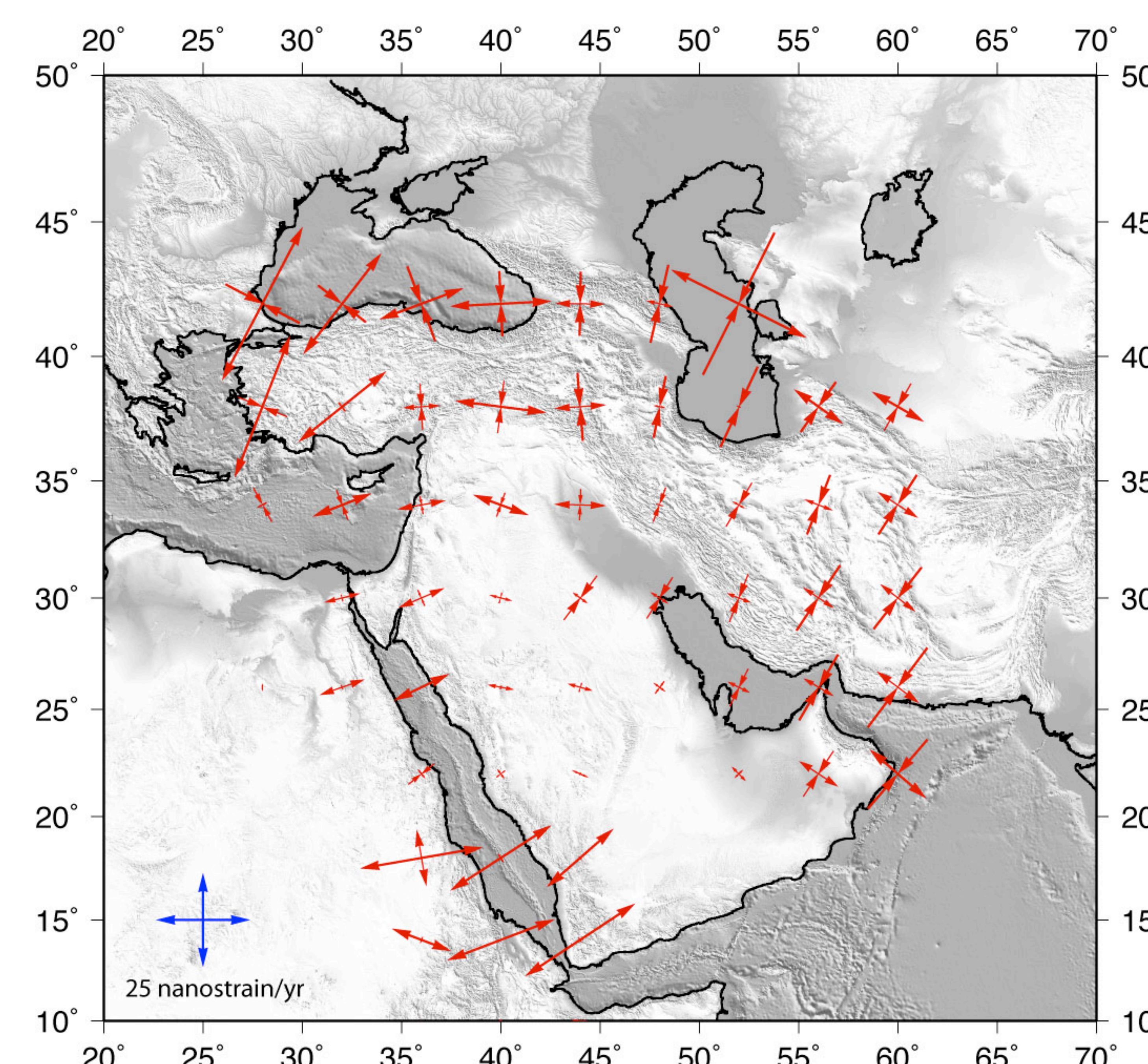


Figure 2 GPS velocities and 95% confidence ellipses for the Arabian plate and surrounding areas in an Arabia-fixed reference frame. Velocities with colored uncertainty ellipses were used to determine the Arabia reference frame. Note very small internal deformation of the plate.



## Contemporary GPS versus geologic plate motions

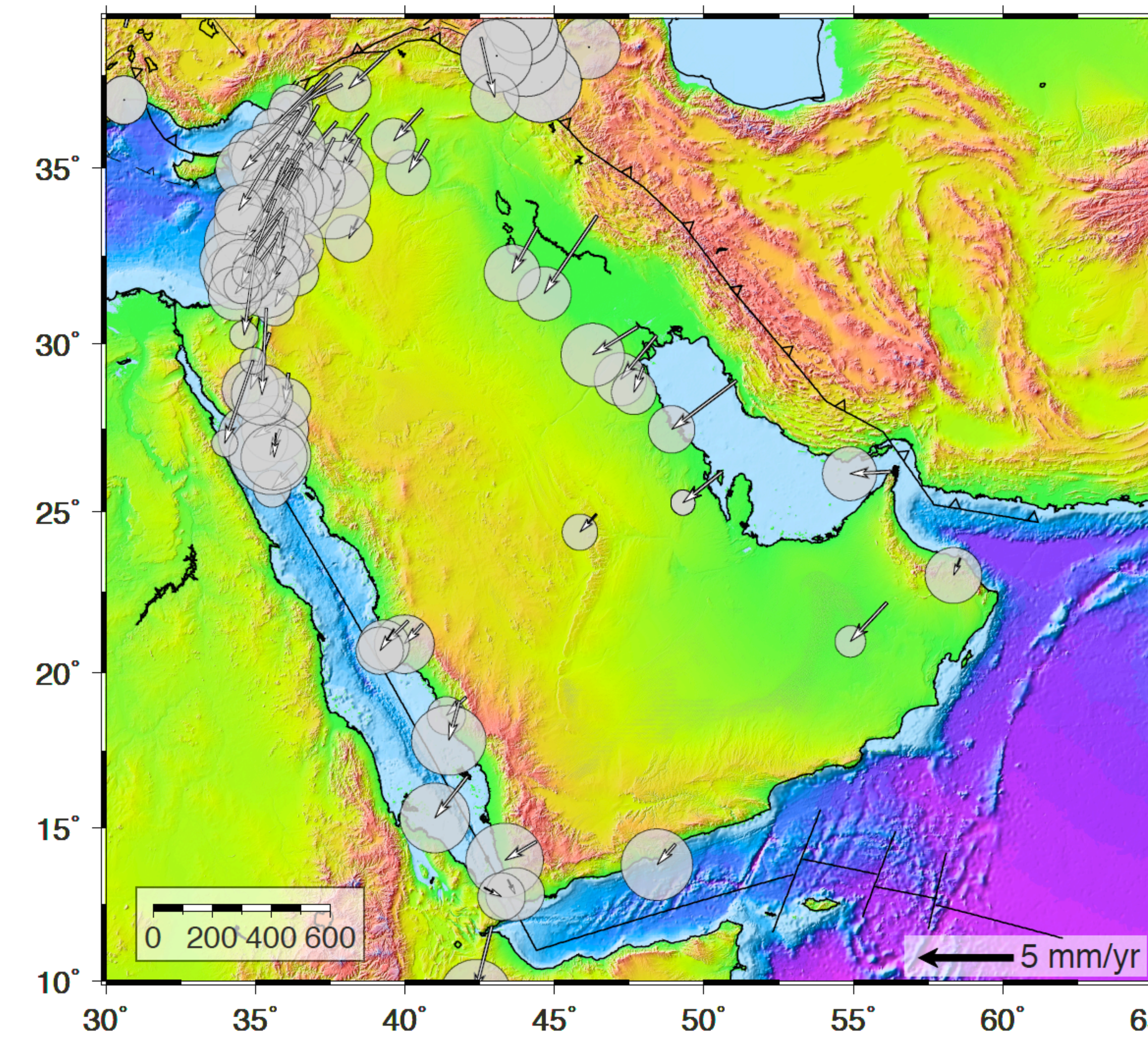


Figure 4 GPS velocities and 95% confidence ellipses for the Arabian Plate with respect to the plate tectonic Euler vector for Arabia based on magnetic anomalies in the Red Sea (Chu and Gordon, 1998). All sites have small westward motions (note scale) indicating slower GPS than plate tectonic (3 Ma) plate motion. Stations in the eastern and central part of the plate show significant westward motion suggesting ~E-W compressional strain not resolvable in the broad scale strain rate estimates (Figure 3).

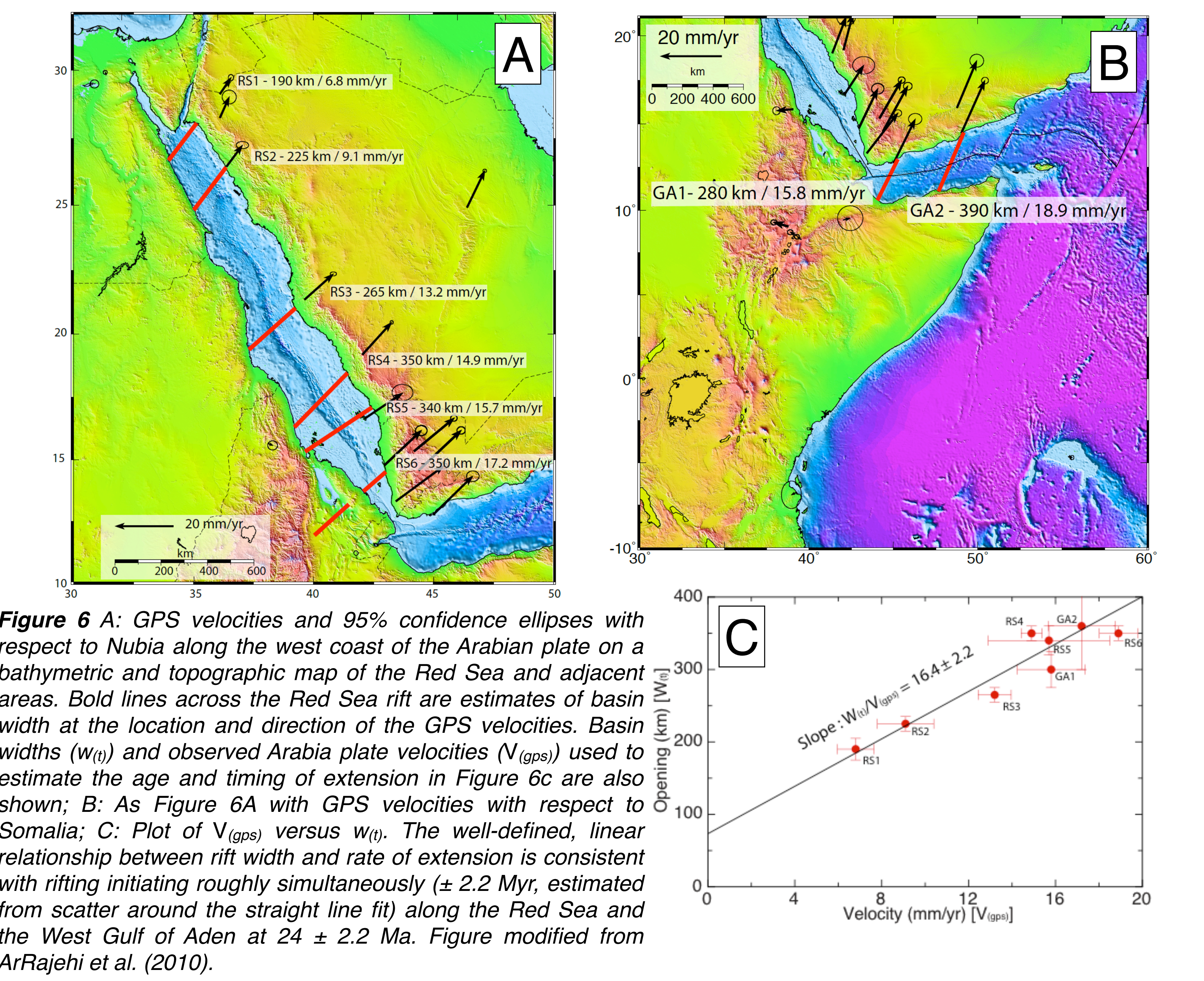


Figure 6 A: GPS velocities and 95% confidence ellipses with respect to Nubia along the west coast of the Arabian plate on a bathymetric and topographic map of the Red Sea and adjacent areas. Bold lines across the Red Sea rift are estimates of basin width at the location and direction of the GPS velocities. Basin widths ( $w(t)$ ) and observed Arabia plate velocities ( $V_{(gps)}$ ) used to estimate the age and timing of extension in Figure 6c are also shown; B: As Figure 6A with GPS velocities with respect to Somalia; C: Plot of  $V_{(gps)}$  versus  $w(t)$ . The well-defined, linear relationship between rift width and rate of extension is consistent with rifting initiating roughly simultaneously ( $\pm 2.2$  Myr, estimated from scatter around the straight line fit) along the Red Sea and the West Gulf of Aden at  $24 \pm 2.2$  Ma. Figure modified from ArRajehi et al. (2010).

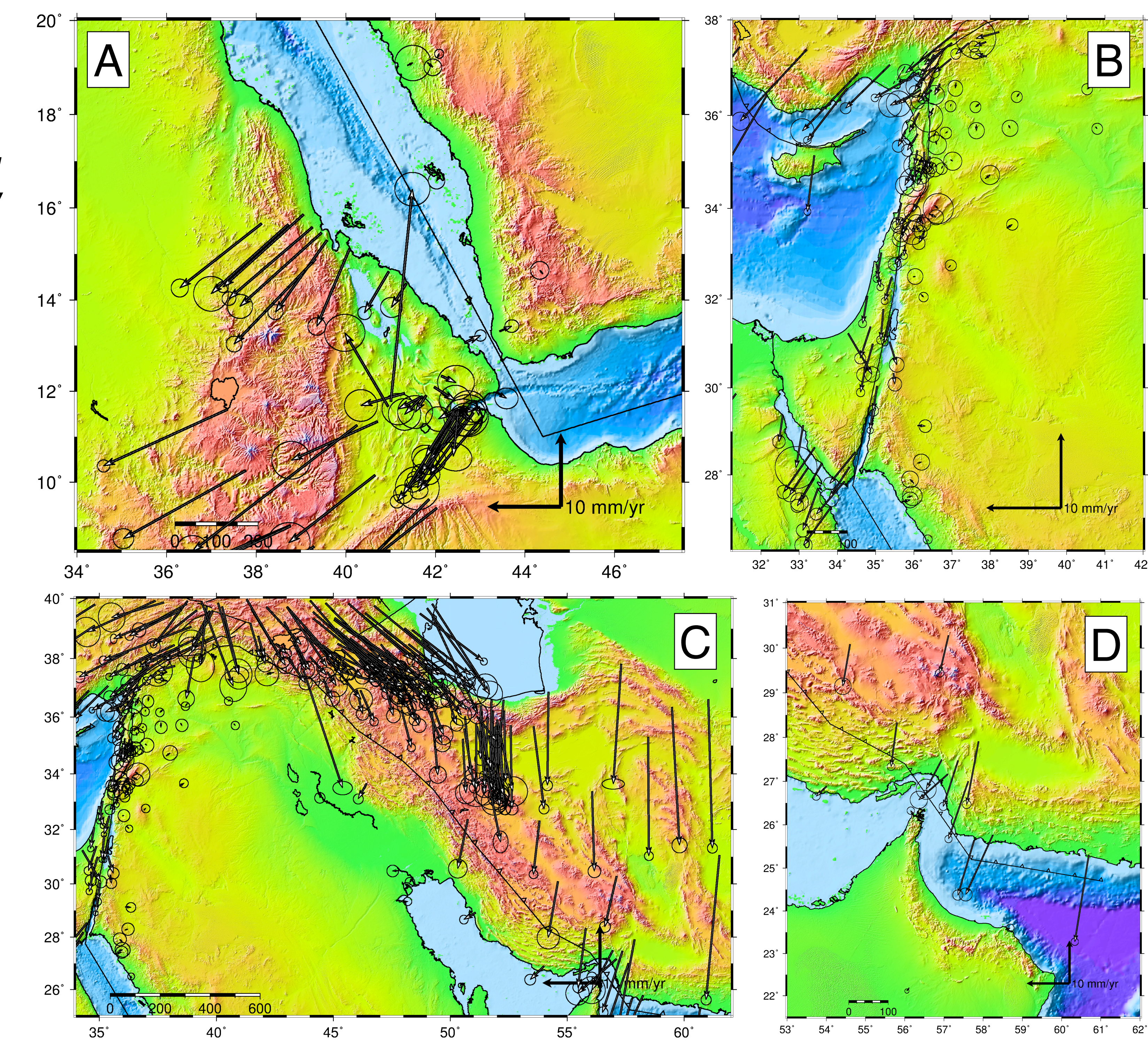


Figure 7 GPS velocities around the boundary of the Arabian Plate. A: Southern Red Sea/Afar Triple junction with respect to Nubia; B: Northern Red Sea/Dead Sea Fault with respect to Arabia (Data courtesy of Francisco Gomez and collaborators); C: Northern Arabia plate boundaries (East Anatolian Fault, Zagros fold and Thrust Belt); D: Oman-Makran subduction.

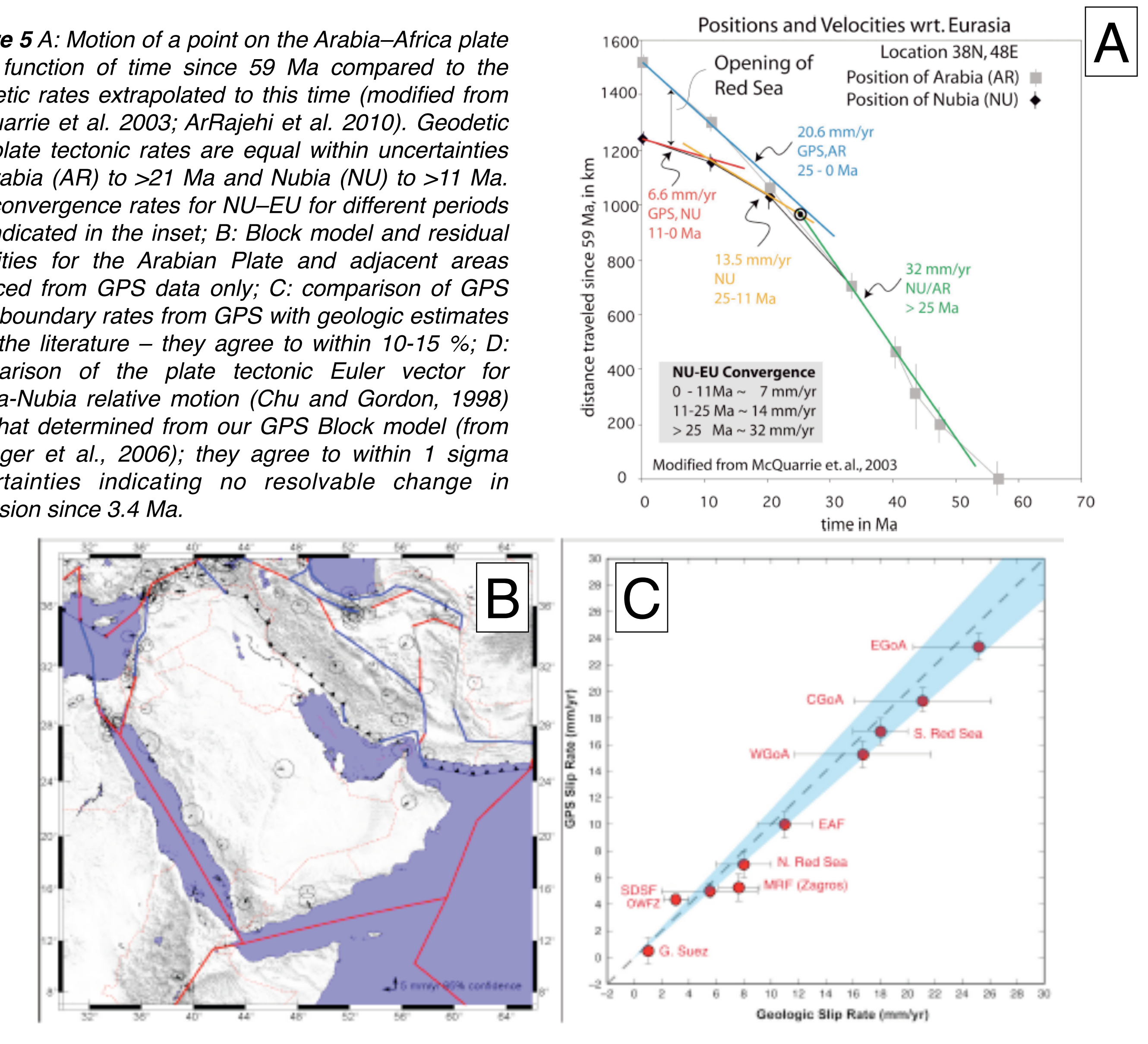


Figure 5 A: Motion of a point on the Arabia-Africa plate as a function of time since 59 Ma compared to the geodetic rates extrapolated to this time (modified from McQuarrie et al. 2003; ArRajehi et al. 2010). Geodetic and plate tectonic rates are equal within uncertainties for Arabia (AR) to >21 Ma and Nubia (NU) to >11 Ma. The convergence rates for NU-EU for different periods are indicated in the inset; B: Block model and residual velocities for the Arabian Plate and adjacent areas deduced from GPS data only; C: comparison of GPS plate boundary rates from GPS with geologic estimates from the literature - they agree to within 10-15 %; D: comparison of the plate tectonic Euler vector for Arabia-Nubia relative motion (Chu and Gordon, 1998) and that determined from our GPS Block model (from Reilinger et al., 2006); they agree to within 1 sigma uncertainties indicating no resolvable change in extension since 3.4 Ma.

D	Lat (°N)	Long (°E)	Rate (°/Ma ccw)	Ref
	31.7 ± 0.2	24.6 ± 0.3	0.37 ± 0.01	ts
	31.5 ± 1.2	23.0 ± 2.7	0.40 ± 0.05	chu